Nano World Journal

https://doi.org/10.17756/nwj.2023-s2-073

Research Article

Open Access

Efficiency in Optimizing the Pre-treatment Process in Water Desalination

Mariem Ennouhi[1*], Sanaa El Aggadi[2*], Walid Belmaghraoui[1], Mohammed Dahhou[2], Laila Azzouzi1, Amale Boutakiout[2] and Mohammed Alaoui El Belghiti[1]

[1]*Laboratory of Spectroscopy, Molecular Modeling, Materials, Nanomaterials, Water and Environment, CERN2D, Faculty of Sciences, Mohammed V University, Rabat, Morocco*

[2]*Laboratory of Materials, nanotechnologies and Environment, Faculty of Sciences, Mohammed V University in Rabat, 4 Avenue Ibn Battouta, BP:1014, Rabat, Morocco*

[*]Correspondence to:

Mariem Ennouhi
Laboratory of Spectroscopy, Molecular Modeling, Materials, Nanomaterials, Water and Environment, CERN2D, Faculty of Sciences,
Mohammed V University, Rabat, Morocco.
E-mail: mariem.ennouhi90@gmail.com

Sanaa El Aggadi
Laboratory of Spectroscopy, Molecular Modeling, Materials, Nanomaterials, Water and Environment, CERN2D, Faculty of Sciences,
Mohammed V University, Rabat, Morocco.
E-mail: sanaa_elaggadi@um5.ac.ma

Received: July 25, 2023
Accepted: September 27, 2023
Published: September 29, 2023

Citation: Ennouhi M, El Aggadi S, Belmaghraoui W, Dahhou M, Azzouzi L, et al. 2023. Efficiency in Optimizing the Pre-treatment Process in Water Desalination. *Nano World J* 9(S2): S431-S437.

Copyright: : © 2023 Ennouhi et al. This is an Open Access article distributed under the terms of the Creative Commons Attribution 4.0 International License (CCBY) (http://creativecommons.org/licenses/by/4.0/) which permits commercial use, including reproduction, adaptation, and distribution of the article provided the original author and source are credited.

Published by United Scientific Group

Abstract

Membrane fouling is a major challenge in membrane processes. The causes are often specific and depend on the constituents of the feed water, the interaction between feed water quality, the pretreatment process, and the used chemicals. This study aims to investigate the effect of pre-treatment on membrane fouling. Various studies were carried out to identify the reasons for membrane fouling: membrane autopsy and pretreatment optimization. The results of the membrane autopsy by scanning electron microscopy/energy-dispersive X-ray spectroscopy (SEM/EDS) revealed that the main causes of membrane fouling are: calcium carbonate ($CaCO_3$; 38.70%), aluminum oxide (Al_2O_3; 17.42%), and barium sulfate ($Ba(SO_4)_2$; 15.23%). The results of the pretreatment optimization allowed to significantly reduce the residual aluminum concentration and the clogging index after the 5 µm cartridge filters. Likewise, it allows to decrease the clogging rate of reverse osmosis membranes.

Keywords

Desalination, Reverse osmosis, Brackish water, Fouling, Coagulation-flocculation

Introduction

The availability of fresh water is facing challenges in various regions worldwide due to factors such as population migration, industrial expansion, climate change, and drought [1, 2]. Despite the fact that 71% of the Earth's surface is comprised of water, primarily in the form of seawater and ocean water, with ice caps at the poles [1, 3], the availability of potable water remains limited, as 97% of the world's water is too saline for consumption [1, 3]. To mitigate the rising demand for fresh water, various strategies have been employed, including water recycling and seawater desalination [2, 3]. Among the techniques used to address the issue of salinity, membrane technologies are considered to be the most widespread and effective [4, 5].

Projections for 2030 indicate a nearly 40% improvement in the world's water intake from available and unidentified water sources, resulting in increased water demand [6]. As drinking water resources quickly become deplorable, it has become extremely important to implement additional water treatment strategies that are effective and inexpensive to meet our evolving water needs. Therefore, the requirement for technological advances to enable innovative desalination and wastewater and drinking water treatment technologies cannot be overstated [7]. The transformation of brackish water, seawater, and wastewater into drinking water requires higher water treatment.

Desalination now becomes a main method to produce drinking water [6]. Desalination is a general term for the process of removing salt from water to produce fresh water [7, 8]. The major problem that limits this process at the plant level is the clogging of the membranes. It is a harmful phenomenon that results in less efficient systems and reduces the reliability of membrane processes [8, 9], thus increasing energy demand, cleaning frequency, chemical consumption, membrane replacement, and high water treatment cost [9, 10]. In this regard, it is necessary to optimize the pretreatment process in order to avoid clogging and to achieve a successful desalination system [11, 12].

The objective of this research paper is to optimize the conventional pretreatment process as a case study in the treatment plant of the city of Khenifra in Morocco. We will utilize the response surface methodology to determine the optimal coagulant dosage for improved desalination outcomes.

Materials and Method

Desalination plant process

In 2013, Morocco established its first surface water treatment plant in Khenifra, which incorporates a conventional treatment process with a reverse osmosis (RO) component (Figure 1) [13, 14]. The facility, which is supplied by the Oum Rbiâa river [14], is designed to meet the region's drinking water needs until 2030, with a daily production capacity of 36,290 cubic meters ($m^3.d^{-1}$) of water. The water from the Oum Rbiâa river is characterized by significant fluctuations in total dissolved solids and elevated levels of chlorides due to its geological origin [15, 16].

The treatment process at the Khenifra plant begins with pre-treatment through a circular scraper settling method, which reduces suspended solids to values less than 2 g/L with the addition of polymer. The next stage is a multiflo system, which includes coagulation with aluminum sulphate, flocculation with anionic polymer, and lamellar decantation, followed by filtration through sand filters. The desalination process involves a microfiltration unit to remove particles larger than 5 µm and to protect the high-pressure pumps. The water is acidified with sulfuric acid (H_2SO_4) to bring the pH to 6.9, preventing $CaCO_3$ precipitation. A sequestering agent is injected upstream of the microfilters to minimize the formation of complexes on the membranes, and sodium bisulfite is added to de-chlorinate the water. All used materials are nanoscale materials.

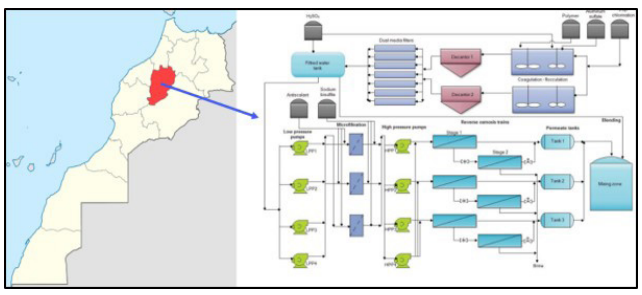


Figure 1: Flow chart of the Khenifra desalination plant [17].

The RO unit consists of three membrane trains belonging to the FILMTEC family. Finally, the water is demineralized through mixing with filtered water and the addition of lime water [18].

RO membrane

Description of the RO membrane

The RO membrane employed is the FilmTec™ XLE440, which is part of the FILMTEC™ FT30 membrane family (Figure 2). The thin-film composite membrane is composed of three layers: a polyester support web, a microporous polysulfone interlayer, and an ultra-thin polyamide barrier layer on the upper surface. Each layer is tailored to meet specific requirements.

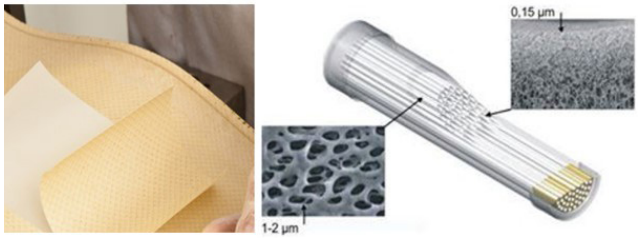


Figure 2: RO membrane.

Characterization of RO membrane

After the fouling experiment, the foulants present on the RO membranes were analyzed. A SEM (LEO1501) was utilized to observe the microscopic surface morphologies, and EDS was conducted to reflect the elemental distribution, particularly of calcium and magnesium. Furthermore, an FTIR (Fourier transform infrared) spectrometer was employed to identify the functional groups present in the foulants.

Flocculation experiment

The flocculation test was performed in the laboratory using a jar test and consisted of three phases: a fast agitation phase of 120 rpm for 2 min, a slow agitation phase of 40 rpm for 20 min, and a decantation phase for 30 min. Raw water was acidified with H_2SO_4 at a concentration of 10 g/L to reduce the pH and attain the optimal pH value, which corresponded to the minimum residual aluminum. The settling process was monitored, and a sample was taken, avoiding any possible suspension of the formed floc. The parameters of pH, turbidity, and residual aluminum were then determined.

Aluminum sulphate solution preparation

A solution of aluminum sulphate ($Al_2(SO_4)_3$) was prepared by dissolving 10 g in 1 L of distilled water. Each milliliter of the solution corresponds to a treatment rate of 10 mg/L. The mud produced from the settling step in the treatment process was used in the flocculation phase. The concentration of suspended matter was determined by filtering 5 ml of the solution through a paper filter with 5 µm porosity.

Methodology

In this study, the response surface methodology (RSM) was used to optimize the pretreatment process based on residual aluminum, utilizing the Doehlert design. RSM is a

collection of mathematical and statistical techniques that fit a polynomial equation to experimental data to make statistical predictions. The Doehlert design was chosen for its advantages over other designs, such as central composite design or Box-Behnken design, including a reduced number of experiments, flexibility in assigning levels to variables, and higher efficiency compared to other designs. The two parameters studied were the concentration of $Al_2(SO_4)_3$ coagulant and pH.

Results and Discussion

The quality of the raw water

The quality of the raw water at the Khenifra plant is notable for its high mineral content and high concentrations of chloride and turbidity. The treatment process at the station utilizes $Al_2(SO_4)_3$ as the aluminum-based coagulant, which can lead to residual aluminum in the water that could potentially clog the reverse osmosis membrane if the process is not optimized. In accordance with the Moroccan standards for drinking water quality outlined in NM.03.7.001 (2006) [19], the maximum permissible level of aluminum in drinking water is 0.20 mg/L. Furthermore, for treatment systems that include a membrane process for demineralization, it is necessary to meet the requirements of the membrane manufacturer and aim for an aluminum content of less than 0.05 mg/L in the membrane feed water. The results of a jar test conducted on a sample of the raw water can be found in table 1.

Table 1 presents the results of a jar test performed on a raw water sample, which indicates that the optimal dose of $Al_2(SO_4)_3$ to achieve the lowest turbidity (0.91 NTU) is around 40 mg/L. This dose corresponds to a pH value of 7.39 and a residual aluminum concentration of 0.18 mg/L. Elevating the $Al_2(SO_4)_3$ dose to 70 mg/L results in a turbidity of 1.25 NTU for the treated water and a residual aluminum content of 0.11 mg/L. This phenomenon is attributed to the decrease in pH to around 7.1 and can be linked to the hydrolysis of aluminum [20, 21]. These findings demonstrate the correlation between pH and residual aluminum, with a decrease in pH resulting in a reduction of residual aluminum. While this content complies with the Moroccan drinking water quality standards (NM.03.7.001 (2006)) [19], it still exceeds the recommendations of the RO membrane manufacturers, which could lead to clogging of the membranes. Thus, it is essential to thoroughly evaluate the RO membrane.

RO performance assessment

Figure 3, figure 4, figure 5, figure 6, and figure 7 show the performance of the RO unit from January 2017 to December 2017, during this period we mainly analyzed the fluctuation of the feed pressure, the differential pressure, the product flow rate, the conductivity of permeate, temperature, and feed conductivity. The purpose of monitoring the plant is to provide details that allow corrections to reduce fouling problems or, ideally, to anticipate fouling [22].

As depicted in figure 3, the feed pressure varied significantly, with a gradual and notable rise due to the osmotic pres-

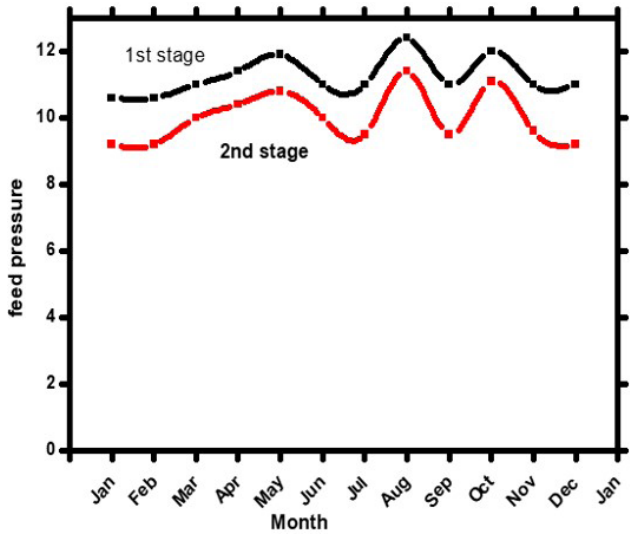


Figure 3: Feed pressure evolution.

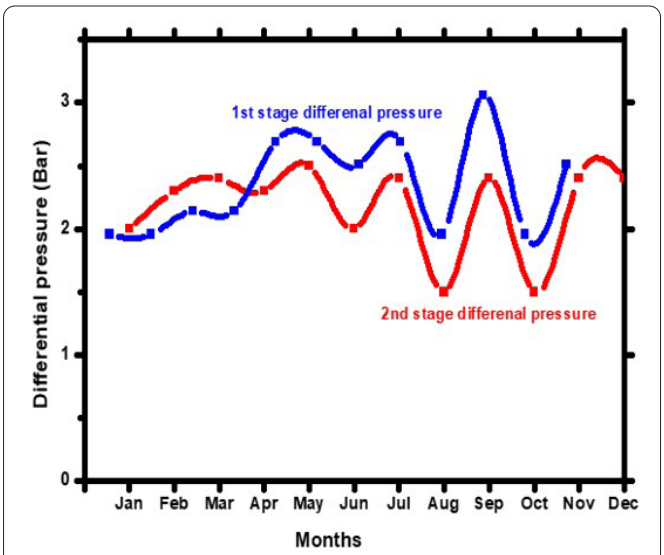


Figure 4: Differential pressure evolution.

Table 1: Results of the jar-test.

Flocculation	Coagulant dose (mg/L)	10	15	20	30	40	50	60	70
	Time to onset of the flocs (min)	1	1	1	1	1	1	1	1
	Aspect of flocs	Good	Good	Good	Good	Good	Good	Good	Good
	Decantation rate	Fast	Fast	Fast	Fast	Fast	Fast	Fast	Fast
After 30 min of setting	pH	7.7	7.59	7.55	7.45	7.39	7.23	7.17	7.1
	Turbidity (NTU)	1.90	1.28	1.2	1.06	0.91	1	1.2	1.25
	Residual aluminum (mg/L)	0.35	0.32	0.28	0.2	0.18	0.13	0.14	0.11
Raw water quality: pH = 8.2, Turbidity = 3 NTU, Residual aluminum = 0 mg/L.									

sure, which rose as the salt concentration of the feed water increased [23]. The first stage saw a rise in feed pressure from approximately 11.1 to 12.8 bar, while the second stage saw a rise from approximately 9.2 to 10.6 bar. During this time, both stages also experienced an increase in pressure difference, as shown in figure 4. However, the permeate flow remained stable across both stages due to the high-pressure pump's automatic regulation. Figure 5 shows that the conductivity of the feed water increased significantly in the first stage and slightly in the second stage, likely due to the increased salt concentration. The influence of seasonal changes in raw water temperature on the supply pressure of the 1st and 2nd stages is illustrated in figure 6.

During the initial stages of plant commissioning, the raw water temperature was around 17.2 °C, and the supply pressure for the 1st and 2nd stages were 11.1 and 9.2 bar, respectively. After approximately two months of operation, the temperature gradually decreased to a minimum of 11.2 °C, resulting in a corresponding gradual increase in the supply pressure of both stages to 12.8 and 10.5 bars (Figure 3). This increase in pressure was a result of the decrease in supply temperature, which altered the structure and physical properties of the membrane.

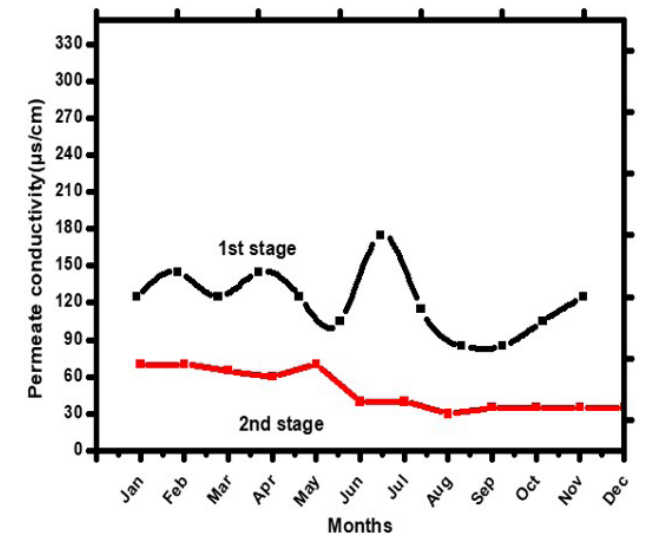


Figure 5: Permeate conductivity evolution.

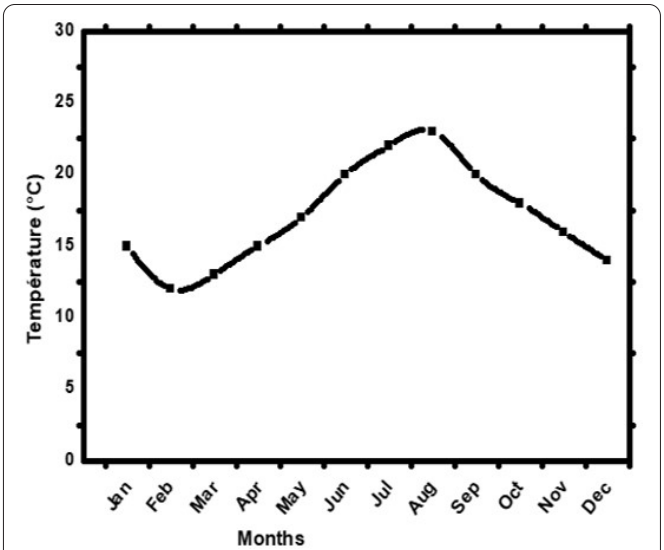


Figure 6: Feed water temperature seasonal variation.

The fluctuation of the conductivity of the plant's feed water is depicted in figure 7. The conductivity showed substantial seasonal changes, with an increase to 2512.3 µS/cm during the summer due to the rise in temperature resulting in water evaporation [24]. In contrast, the conductivity was reduced to 1333.8 µS/cm during the winter as a result of dilution caused by rain. This increase in conductivity may have both short-term and long-term effects on the membrane.

In the short term, the quality of the permeate and production capacity will gradually decline. In the long term, if the anti-scalant dosage is not adjusted, the membranes will experience severe scaling or even irreversible fouling, leading to a decrease in membrane production.

The feed water experiences strong seasonal fluctuations in temperature and conductivity that result in the precipitation of salts on the membrane surface and scaling of the membranes, thus necessitating an evaluation of the RO membrane [25, 26].

Characterization of RO membrane

SEM images show the morphological appearance of the fouling as well as the extent of the layer thickness (Figure 8). The deposits were unevenly distributed over the membrane surface. It is also noticeable that the area outside the feed spacer is more loaded than the other area as shown in figure 8. SEM and EDS inspection confirms the diversity of the fouling composition layer on the membrane surface and the membrane surface and provides insight into the nature and method of layer development. As shown in figure 8, a typical fouling membrane surface is composed of particulate matter embedded in an apparently amorphous matrix [24]. The associated EDS analyses revealed the presence of calcium in large quantities, which is responsible for the formation of scale.

The aluminum and oxygen peaks are likely due in part to organic and/or biological materials. The high levels of aluminum and oxygen in the particles suggest that they were

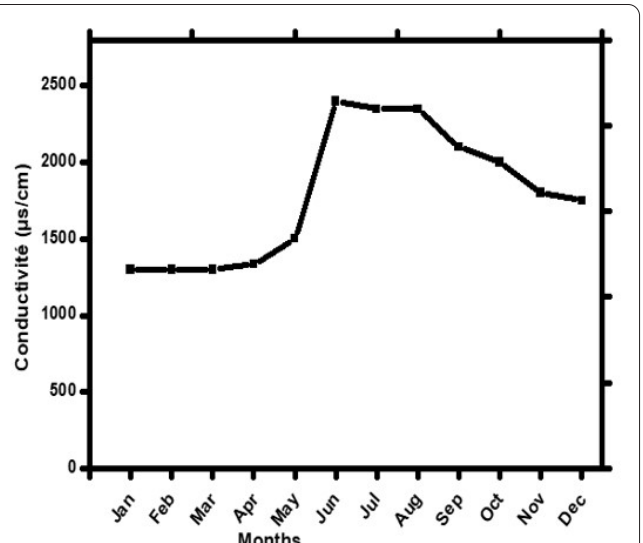


Figure 7: Feed water conductivity seasonal fluctuations.

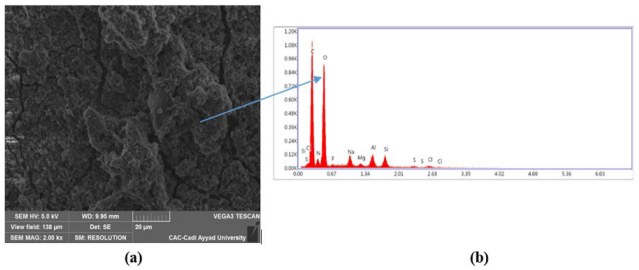


Figure 8: (a) SEM images of a RO membrane structure x2000 and **(b)** EDS spectrum result.

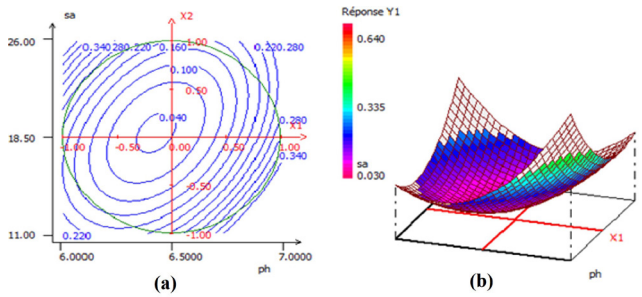


Figure 9: Isoreponse curve **(a)** and the response surface **(b)** of residual aluminum depending on the pH and $Al_2(SO_4)_3$.

primarily aluminum oxide, which are common pollutants in RO operations [27]. The use of $Al_2(SO_4)_3$ as a coagulant prior to RO treatment could also increase the concentration of aluminum in the RO feed, which could provide evidence of aluminum dioxide in the fouling layer. Therefore, the need to optimize the pre-treatment.

Determination of the pH and the optimal dose of $Al_2(SO_4)_3$

The optimization of the process parameters was performed using the experimental design method. The Doehlert matrix proposed by Doehlert (1970) [27] was utilized. The initial focus of the study was on two variables, the pH (X1) and the dose of $Al_2(SO_4)_3$ (SA = X2). The Doehlert model with two variables forms a regular hexagonal shape, with each corner and the center representing a separate experiment. The results of the study enabled the expression of the residual aluminum optimization as a function of both pH and $Al_2(SO_4)_3$ dose through equation 1.

$$Y = 0.024 + 0.051X_1 - 0.030X_1^2 + 0.155X_2^2 - 0.138X_1X_2 \quad (1)$$

The predicted residual aluminum values (Y), using equation 1, are given in table 2.

The Doehlert experimental matrix was utilized [27] to optimize the pH and the dose of $Al_2(SO_4)_3$ through the application of an experimental design method. The study focused on two variables: pH (X1) and the dose of $Al_2(SO_4)_3$ (SA = X2). The results were expressed as the optimization of residual aluminum as a function of pH and $Al_2(SO_4)_3$ dose through equation 1.

Figure 9 displays the isoresponse curve (a) and the response surface curve (b), which demonstrate the impact of pH and $Al_2(SO_4)_3$ dose on residual aluminum reduction. The interaction between these two factors highlights that adjusting them correctly can lead to optimal residual aluminum levels. The minimum residual aluminum value of 0.03 mg/L was obtained near the central values of pH (6.5) and $Al_2(SO_4)_3$ dose (18.5 mg/L). This meets the requirement for membrane suppliers (Al < 0.05 mg/L).

Considering the raw water quality, including turbidity and suspended load, the dose of $Al_2(SO_4)_3$ needs to be adjusted. To optimize residual aluminum content, it is necessary to adjust the pH to a value close to 6.5 by adding H_2SO_4.

Evaluation of pretreatment performance

Figure 10 and figure 11 show the evolution of the residual aluminum of the filtered and microfiltered water before and after optimization.

In figure 10, the fluctuation in residual aluminum content in the filtered water is depicted. The residual aluminum ranged between 0.05 to 0.12 mg/L, with an average of 0.07 mg/L during the observation period. To examine the impact of 5 µm cartridges on residual aluminum, monitoring was carried out on both filtered and microfiltered water. The results shown in figure 11 reveal that there was a substantial reduction of residual aluminum in the filtered water after passing through the microfiltration process, a decrease of approximately 37%. This demonstrates the effectiveness of the 5 µm cartridges in reducing the residual aluminum concentration prior to the RO membranes.

Conclusion

In conclusion, this study aimed to investigate the influence of coagulation flocculation pretreatment on the fouling of the RO membrane in a treatment station in the

Table 2: Experimental design to two factors with the experimental values and the values predicted from residual aluminum.

Experiment number	X_1 (pH)	X_2 $Al_2(SO_4)_3$ (mg/L)	Value predicted (y) (mg/L)	Experimental value (y) (mg/L)
1	7	18.5	0.21	0.25
2	6	18.5	0.24	0.24
3	6.8	25	0.20	0.21
4	6.3	12	0.12	0.08
5	6.8	12	0.33	0.39
6	6.3	25	0.16	0.14
7	6.5	18.5	0.03	0.04
8	6.5	18.5	0.03	0.04
9	6.5	18.5	0.03	0.04

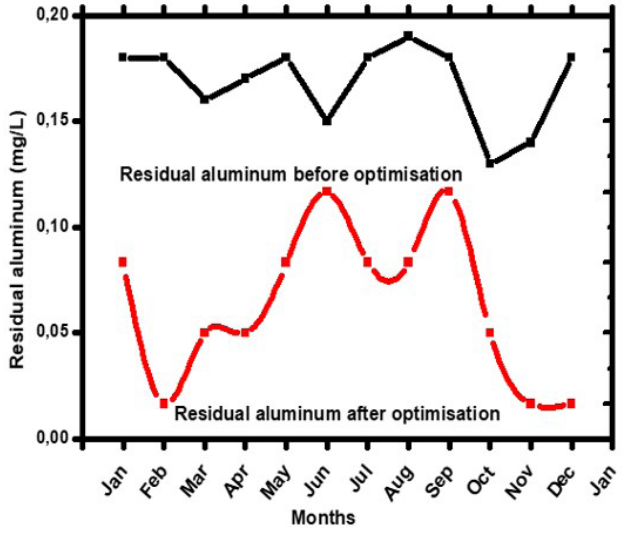


Figure 10: Evolution of the residual aluminum filtered water before and after optimization.

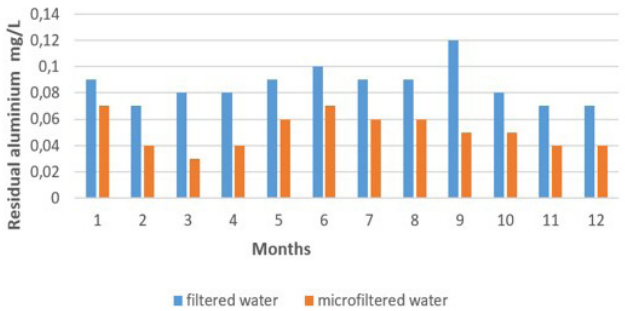


Figure 11: Evolution of the residual aluminum the micro filtered water before and after optimization.

city of Khenifra. Through SEM/EDS analysis, the fouling layer was found to be mainly composed of $CaCO_3$ (38.70%) and Al_2O_3 (17.42%), and large cracks were observed on the surface of the membrane. The RSM was applied to optimize the conventional pretreatment by determining the optimal pH and dose of $Al_2(SO_4)_3$. The results showed that a pH value of 6.5 and $Al_2(SO_4)_3$ concentration of 19 mg/L were optimal in reducing residual aluminum to 0.03 mg/L, which meets the requirements of membrane suppliers. This study highlights the importance of adjusting pH and $Al_2(SO_4)_3$ concentration based on the quality of raw water to optimize pretreatment and reduce fouling of the RO membrane.

Acknowledgements

None.

Conflict of Interest

None.

References

1. Zhao L, Ho WW. 2014. Novel reverse osmosis membranes incorporated with a hydrophilic additive for seawater desalination. *J Membr Sci* 455: 44-54. https://doi.org/10.1016/j.memsci.2013.12.066
2. Aliyu UM, Rathilal S, Isa YM. 2018. Membrane desalination technologies in water treatment: a review. *Water Pract Technol* 13(4): 738-752. https://doi.org/10.2166/wpt.2018.084
3. Burn S, Hoang M, Zarzo D, Olewniak F, Campos E, et al. 2015. Desalination techniques-a review of the opportunities for desalination in agriculture. *Desalination* 364: 2-16. https://doi.org/10.1016/j.desal.2015.01.041
4. Akther N, Sodiq A, Giwa A, Daer S, Arafat HA, et al. 2015. Recent advancements in forward osmosis desalination: a review. *Chem Eng J* 281: 502-522. https://doi.org/10.1016/j.cej.2015.05.080
5. Jiang S, Li Y, Ladewig BP. 2017. A review of reverse osmosis membrane fouling and control strategies. *Sci Total Environ* 595: 567-583. https://doi.org/10.1016/j.scitotenv.2017.03.235
6. Majeed T, Phuntsho S, Jeong S, Zhao Y, Gao B, et al. 2016. Understanding the risk of scaling and fouling in hollow fiber forward osmosis membrane application. *Process Saf Environ Prot* 104: 452-464. https://doi.org/10.1016/j.psep.2016.06.023
7. Chollom MN, Rathilal S, Alfa D, Pillay VL. 2015. The applicability of nanofiltration for the treatment and reuse of textile reactive dye effluent. *Water SA* 41(3): 398-405.
8. Kaplan R, Mamrosh D, Salih HH, Dastgheib SA. 2017. Assessment of desalination technologies for treatment of a highly saline brine from a potential CO_2 storage site. *Desalination* 404: 87-101. https://doi.org/10.1016/j.desal.2016.11.018
9. Bush JA, Vanneste J, Cath TY. 2016. Membrane distillation for concentration of hypersaline brines from the Great Salt Lake: effects of scaling and fouling on performance, efficiency, and salt rejection. *Sep Purif Technol* 170: 78-91. https://doi.org/10.1016/j.seppur.2016.06.028
10. Wang Q, Li N, Bolto B, Hoang M, Xie Z. 2016. Desalination by pervaporation: a review. *Desalination* 387: 46-60. https://doi.org/10.1016/j.desal.2016.02.036
11. Kaminski W, Marszalek J, Tomczak E. 2018. Water desalination by pervaporation–comparison of energy consumption. *Desalination* 433: 89-93. https://doi.org/10.1016/j.desal.2018.01.014
12. Khazaei A, Mohebbi V, Behbahani RM, Ramazani SA. 2018. Energy consumption in pervaporation, conventional and hybrid processes to separate toluene and i-octane. *Chem Eng Process Process Intensif* 128: 46-52. https://doi.org/10.1016/j.cep.2018.04.009
13. Toth AJ, Andre A, Haaz E, Mizsey P. 2015. New horizon for the membrane separation: combination of organophilic and hydrophilic pervaporations. *Sep Purif Technol* 156: 432-443. https://doi.org/10.1016/j.seppur.2015.10.032
14. Boulahfaa H, Belhamidia S, Elhannounia F, Taky M, Hafsib M, et al. 2020. Pretreatment process optimization and reverse osmosis performances of a brackish surface water demineralization plant, Morocco. *Desalin Water Treat* 206: 189-201. https://doi.org/10.5004/dwt.2020.26297
15. Boulahfa H, Belhamidi S, Elhannouni F, Taky M, El Fadil A, et al. 2019. Demineralization of brackish surface water by reverse osmosis: the first experience in Morocco. *J Environ Chem Eng* 7(2): 102937. https://doi.org/10.1016/j.jece.2019.102937
16. Hanchate N, Kulshreshtha P, Mathpati CS. 2019. Optimization, scale-up and cost estimation of dehydration of ethanol using temperature swing adsorption. *J Environ Chem Eng* 7(2): 102938. https://doi.org/10.1016/j.jece.2019.102938
17. Ennouhi M, El Aggadi S, Hasnaoui L, El Azzouzi M, El Hourch A. 2021. Relationship between reverse osmosis membrane fouling and pretreatment in the Khenifra city plant in Morocco. *Ann Romanian Soc Cell Biol* 25(6): 12814-12819.
18. Boulahfa H, Belhamidi S, Elhannouni F, Taky M, El Fadil A, et al. 2019. Impact of the raw water seasonal variations on the reverse osmosis performance: Khenifra Plant, Morocco. *J Water Environ Technol* 17(5): 359-374. https://doi.org/10.2965/jwet.19-028

19. Tahaikt M, Haddou AA, El Habbani R, Amor Z, Elhannouni F, et al. 2008. Comparison of the performances of three commercial membranes in fluoride removal by nanofiltration. Continuous operations. *Desalination* 225(1-3): 209-219. https://doi.org/10.1016/j.desal.2007.07.007

20. Kim J, Park K, Yang DR, Hong S. 2019. A comprehensive review of energy consumption of seawater reverse osmosis desalination plants. *Appl Energy* 254: 113652. https://doi.org/10.1016/j.apenergy.2019.113652

21. Zolfaghari G, Kargar M. 2019. Nanofiltration and microfiltration for the removal of chromium, total dissolved solids, and sulfate from water. *MethodsX* 6: 549-557. https://doi.org/10.1016/j.mex.2019.03.012

22. Kim J, Hong S. 2018. Optimizing seawater reverse osmosis with internally staged design to improve product water quality and energy efficiency. *J Membr Sci* 568: 76-86. https://doi.org/10.1016/j.memsci.2018.09.046

23. Rashidi MM, Mahariq I, Murshid N, Wongwises S, Mahian O, et al. 2022. Applying wind energy as a clean source for reverse osmosis desalination: a comprehensive review. *Alexandria Eng J* 61(12): 12977-12989. https://doi.org/10.1016/j.aej.2022.06.056

24. Badruzzaman M, Voutchkov N, Weinrich L, Jacangelo JG. 2019. Selection of pretreatment technologies for seawater reverse osmosis plants: a review. *Desalination* 449: 78-91. https://doi.org/10.1016/j.desal.2018.10.006

25. Fritzmann C, Löwenberg J, Wintgens T, Melin T. 2007. State-of-the-art of reverse osmosis desalination. *Desalination* 216(1-3): 1-76. https://doi.org/10.1016/j.desal.2006.12.009

26. Sharqawy MH, Zubair SM. 2011. Second law analysis of reverse osmosis desalination plants: an alternative design using pressure retarded osmosis. *Energy* 36(11): 6617-6626. https://doi.org/10.1016/j.energy.2011.08.056

27. Lachheb A, Belhamidi S, Zouhri N, Idrissi YA, Hafsi M, et al. 2016. Performances analysis of the reverse osmosis desalination plant of brackish water used for drinking water: Tagounite, Morocco. *J Chem Pharm Res* 8(4): 119-129.